

IMPLEMENTATION OF A PLATE-TYPE FUEL MODEL TO A MULTI-PHYSICS CODE AND BENCHMARK MODELING OF SPECIAL POWER EXCURSION REACTOR TESTS

P. Liu*, D. Wilhelm, A. Rineiski, F. Gabrielli, W. Maschek

Forschungszentrum Karlsruhe, Institute for Nuclear and Energy Technologies,
P.O.Box 3640, D-76021 Karlsruhe, Germany

* ping.liu@iket.fzk.de

G. B. Bruna

Reactor Safety Division, French Institute for Radioprotection and Nuclear Safety (IRSN)

B.P. 17, 92262 Fontenay aux Roses Cedex, France

giovanni.bruna@irsn.fr

ABSTRACT

SIMMER-III, a neutronics and thermal-hydraulics coupled code, was originally developed for core disruptive accident analyses of liquid metal cooled fast reactors. Because of the code's versatility in investigating scenarios of core disruption, the code has also been extended to the simulation of transients in thermal neutron systems such as the criticality accident at the JCO fuel fabrication plant, and in recent years applied to water-moderated thermal research reactors. Originally, SIMMER-III code considered only cylindrical fuel pin geometry. Therefore, implementation of a plate-type fuel model to the SIMMER-III code is of importance for the analysis of research reactors with this type of fuel. Furthermore, validation of the SIMMER-III modeling of light water-cooled thermal reactor transients caused by reactivity insertion is of necessity. This paper will firstly deal with the implementation of a new fuel model in SIMMER-III. On the basis of the original cylindrical pin model, a plate-type model has been developed and implemented. Verification on this new model indicates that it can well simulate the temperature profile in the fuel. Secondly, Special Power Excursion Reactor Tests (SPERT) has been simulated. The obtained results are qualitatively reasonable, while the negative feedback modeling just before and after the peak power point needs further investigation. As an example, the case of SPERT I D-12/25 with the shortest reactor period of 3.2 msec will be presented and discussed in this paper.

Key Words: SIMMER-III, Plate-type fuel pin, Reactivity insertion, SPERT, Reactor safety

1. INTRODUCTION

SIMMER-III [1, 2], a two-dimensional, multi-velocity-field, multi-phase, multi-component, Eulerian, fluid-dynamics code coupled with a fuel-pin model and a space- and energy-dependent neutron transport kinetics model, is an advanced computer code used to predict the coupled neutron and fluid-dynamics behavior of liquid metal cooled fast reactors (LMFRs) [3-5] and accelerator driven systems (ADSs) [6] especially during the core disruptive accident (CDA). Development of SIMMER-III has successfully reached a milestone by now with the completion of all physical models originally intended for simulating sequences of CDAs in LMFRs and ADSs. It has been applied to many kinds of ADS and LMFR safety analyses, which have proved

its general validity and flexibility. Meanwhile, in order to apply it reliably to safety analyses of other reactors, the assessment and improvement of the code is still on-going in particular for handling general types of multiphase flow problems.

Apart from the FBRs and ADSs, SIMMER-III has also been successfully applied to the simulation of transients in a thermal neutron system. With a radiolytic gas model implemented, SIMMER-III has well simulated the early burst phase of the so-called JCO accident [7]. In recent years, SIMMER-III has been targeted to special topics in the analyses of light water-cooled research reactors [8, 9], which have a plate-type fuel (plate fuel meat is hereafter also called “fuel pellet”, similar to the traditional cylindrical fuel pin). Initially the SIMMER-III cylindrical fuel pin model [10] has been adopted in the performed simulations. It becomes obviously necessary to implement a plate-type fuel model for reliable application to reactors with this type of fuel. Therefore, on the basis of the original cylindrical pin model, a new plate-type fuel model has been developed and implemented. Verification on this model has been performed for a simplified case, in which the fuel plate temperature profile can be obtained from an analytical solution. A comparison between SIMMER-III simulated result and the analytical solution indicates that the implemented plate-type fuel model can well simulate the temperature profile.

In order to validate the applicability of SIMMER-III to the disruptive transient analysis of the light water cooled reactor, the SPERT I D-12/25 core disruptive tests [11] - induced by reactivity insertion - have been chosen as the benchmark problem for SIMMER-III. In 1962, a series of tests were conducted at SPERT I D-12/25 facility by inserting large reactivity to induce short period power excursions, among which, three tests conducted with reactor periods of 5.0 msec, 4.6 msec and 3.2 msec, respectively, resulted in both thermal distortion of the plate and fuel plate melting. The tests showed that the thermal expansion and steam formation were the effective shutdown mechanisms. First SIMMER-III simulations for these three tests have been performed. As an example, results of the case with a 3.2 msec period will be presented and discussed in this paper.

2. IMPLEMENTATION OF A PLATE-TYPE FUEL MODEL TO SIMMER-III

2.1. The Necessity to Implement a Plate-type Fuel Model

Considering the basic heat conduction equation, where q is the heat per unit volume (W/m^3), T_c is the fuel center temperature, T_w is the fuel surface temperature, k is the thermal conductivity, and r_{cyl} is radius of the cylindrical fuel pin, r_{plate} is the distance from the fuel plate center (r_{plate} equals to half of the total fuel plate thickness δ_{plate}), the Fourier equation yields:

$$q = -k \frac{d^2T}{dr_{plate}^2}, \text{ for the plate} \quad (1)$$

$$q = -k\left(\frac{d^2T}{dr_{cyl}^2} + \frac{dT}{r_{cyl}dr_{cyl}}\right), \text{ for the cylinder} \quad (2)$$

Taking into account that $\frac{dT}{dr_{cyl}} = 0$ and $\frac{dT}{dr_{plate}} = 0$ at $r_{cyl} = r_{plate} = 0$, then the differences between T_c and T_w become:

$$T_c - T_w = \frac{q}{2k} r_{plate}^2, \text{ for the plate} \quad (3)$$

$$T_c - T_w = \frac{q}{4k} r_{cyl}^2, \text{ for the cylinder} \quad (4)$$

Originally the SIMMER-III code dealt with fuel pins only. Therefore, first calculations for a water-moderated research reactor with aluminum plate-type fuel were carried out with this cylindrical model [8, 9]. The transformation from the original plate to the cylinder geometry was done by preserving the pin volume and the wetted surface, as was demonstrated in [8]. This treatment needs a definition of

$$r_{cyl} = 2r_{plate} \quad (5)$$

Substituting Eq. (5) into Eq. (4) and then comparing with Eq. (3), it can be deduced that by adopting a cylindrical geometry for the plate-type fuel, the temperature difference between T_c and T_w becomes twice of that in plate-type geometry when other conditions are the same. This indicates the necessity of introducing a plate-type fuel model into the SIMMER-III code.

2.2. Plate-type Fuel Model

In order to simplify the implementation, the plate-type fuel model has been developed on the basis of the existing code system, especially the original cylindrical fuel pin model. Fig. 1(a) is a view of the cylindrical pin geometry. Two nodes (INT for the fuel interior, S1 for the fuel surface) have been defined for the fuel pellet while another single node (S4) for the cladding. The gap (nf) between the cladding and the fuel pellet is defined as non-flow region whose volume is added to the flow region when the cladding is lost. Detailed modeling description refers to the work of Kamiyama and Kondo [10]. It needs to be pointed out that parameters in SIMMER-III are defined on the basis of per unit volume of each mesh cell.

When it comes to the plate-type fuel, the geometry will be changed to Fig. 1(b). If the fuel plate half-thickness is X_{pin} , the fuel pellet half-thickness is X_{pel} , the thickness of the node S1 is δ_{S1} , and α is the volume fraction, then X_{p0} , X_{p1} , X_{p2} , X_{p3} , X_{p4} , X_{p5} , and X_{p6} shown in Fig.1(b) have the following definitions:

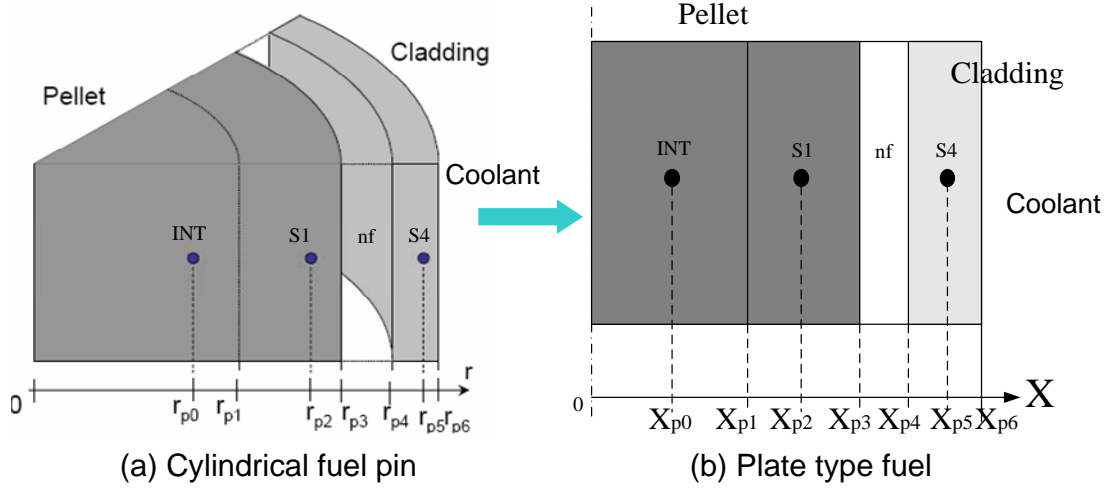


Figure 1. Fuel pin configurations in SIMMER-III.

$$\begin{aligned}
 X_{p6} = X_{pin} = \delta_{plate} / 2, X_{p4} = X_{pin} \frac{\alpha_{INT} + \alpha_{S1} + \alpha_{nf}}{\alpha_{pin}}, X_{p5} = (X_{p6} + X_{p4})/2 \\
 X_{p3} = X_{pel} = X_{pin} \frac{\alpha_{INT} + \alpha_{S1}}{\alpha_{pin}}, X_{p1} = X_{p3} - \delta_{S1}, X_{p2} = (X_{p1} + X_{p3})/2, X_{p0} = (X_{p1})/2 \quad (6)
 \end{aligned}$$

For a plate-type fuel, the surface area of the fuel plate per unit volume is

$$a_{pin} = (\alpha_{INT} + \alpha_{S1}) / X_{p3} = (\alpha_{INT} + \alpha_{S1} + \alpha_{nf} + \alpha_{S4}) / X_{p6} \quad (7)$$

The heat transfer coefficients for the cladding S4 and the fuel surface S1 are

$$h_{S4} = K_s / (X_{p6} - X_{p5}), h_{S1} = K_f / (X_{p3} - X_{p2}) \quad (8)$$

where K_s and K_f are the thermal conductivity of the cladding and the fuel, respectively. Eq. (7) will be used in the heat transfer modeling between the fuel plate and the coolant. The heat transfer coefficient between the cladding S4 and the fuel pellet surface S1 is as follows:

$$h_{S1,S4} = [(X_{p3} - X_{p2}) / K_f + 1/h_{gap} + (X_{p5} - X_{p4}) / K_s]^{-1}, \quad (9)$$

Where h_{gap} is the gap conductance, which can be defined in the input or can be calculated by $h_{gap} = K_{gap} / (X_{p4} - X_{p3})$, K_{gap} is the thermal conductivity in the gap (between the fuel surface and the cladding). The heat transfer coefficient between fuel nodes S1 and INT is defined as:

$$h_{INT,S1} = K_f / (X_{p2} - X_{p0}) \quad (10)$$

The energy conservation equation for the fuel plate heat transfer simulation is:

$$\frac{\partial \alpha_m \rho_m e_m}{\partial t} = h_{m,m-1} a_{m,m-1} (T_{m-1} - T_m) + h_{m+1,m} a_{m+1,m} (T_{m+1} - T_m) + Q_{Hm} + Q_{Nm} \quad (11)$$

where the subscript m stands for one of the three nodes, namely, INT, S1 and S4. Q_{Hm} and Q_{Nm} in Eq. (11) are the energy transfer rates due to heat transfer from fluid and nuclear heating, respectively. The heat transfer coefficients can be calculated by Eqs. (9) and (10) while for the plate-type fuel the heat transfer areas between every two nodes are $a = a_{pin}$. Therefore, the plate type fuel temperature profile can be obtained by solving Eq. (11) together with mass and momentum equations.

2.3 Verification of the Implemented Plate-type Fuel Model

The plate-type fuel model has been verified on the basis of a simplified test case. A total power of 30,000 W which leads to a volumetric power of 8.22819×10^8 W/m³ in the plate-type fuel has been assigned to the test system, which is the same as the research reactor simulation case [9]. The fuel plate including its cladding has a thickness of 4.75 mm while the thickness of the pure fuel pellet is 4.0712 mm. No gap exists between the fuel pellet and cladding. In this verification test, the temperature profile in the fuel plate is the only concern. In order to simplify the verification, a very large heat transfer rate between the fuel plate and the water surrounding it has been assumed, while the fuel pellet and cladding are supposed to have a same thermal conductivity of 10 W/(m·K). All key parameters are listed in Table I.

Table I. Key parameters defined in the plate-type fuel pin modeling test

Parameters	Plate geometry
Total power (W)	30000.
Volumetric power (W/m ³)	8.22819E+08
Pellet volume fraction	0.6789
Clad volume fraction	0.1132
Water	0.2088
X _{pin} (mm)	2.375 (half of the fuel pin thickness)
X _{pel} (mm)	2.0356 (half of the pellet thickness)
Multiplier on the heat transfer between clad and water	100
Pellet thermal conductivity (W/(m·K))	10

The simulation is performed with constant nuclear heat until a steady state is reached. The SIMMER-III code without neutronics part is used, and the nuclear heat is specified by the input. Results of the temperature difference between the fuel center and plate surface are compared to the analytical solution of the steady state Fourier equation. Table II shows the temperature difference. The difference between the SIMMER-III simulated and analytical result is only 2.5 K. Fig. 2 shows the temperature profiles in the X-direction. The difference between T_{INT} and T_{S4} corresponds to the $T_c - T_w$ in Table II. Results listed in Table II and the temperature profile in Fig. 2 show very good agreement between the analytical and SIMMER-III simulated results. Therefore, it is verified that the new implemented plate-type fuel model can well simulate the temperature distribution inside the plate-type fuel.

Table II. Temperature difference between the fuel center and the fuel plate surface

Parameters	Theoretical result	SIMMER-III
Temperature difference ($T_c - T_w$) (K)	$\frac{q}{2k} r^2$	$T_{INT} - T_{S4}$
	170.5	173

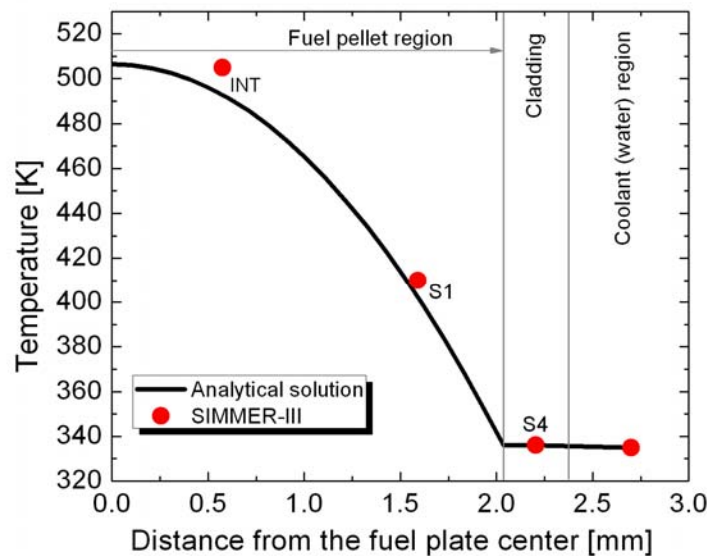


Figure 2. Comparison of the X-direction temperature profile. INT, S1, S4 are the three nodes defined for the fuel plate in SIMMER-III (see Fig. 1).

3. SIMMER-III MODELING OF SPERT I D-12/25 POWER EXCURSION TESTS

3.1. Overview of the SPERT I D-12/25 Power Excursion Tests

In 1962, a series of tests was conducted at SPERT I D-12/25 facility to demonstrate the operational and safety behavior of an aluminum, plate-type, water-moderated, highly-enriched reactor by inserting large reactivity to induce short period power excursions [11]. The SPERT I reactor vessel is an open, unpressurized carbon-steel tank which has a diameter of 304.8 cm and a depth of 487.7 cm. The water level in the reactor vessel was 137.2 cm above the top of the fuel plates. There is no forced coolant circulation through the core.

The test core was comprised of 25 fuel assemblies including 20 standard fuel assemblies, 4 control assemblies and 1 transient assembly, mounted in a 5 x 5 rectangular grid structure as shown in Fig. 3. Each standard fuel assembly contains 12 aluminum-clad (Al 6061) highly enriched, U-Al alloy fuel plates. The fuel meat consists of 23.8 wt% uranium and 76.2 wt% aluminum. The uranium has an isotopic mixture of 93.17 wt% U-235, 1.05 wt% U-234, and 5.78 wt % U-238 [12]. The dimensions of each fuel plate at room temperature are 0.1524 cm x 6.86816 cm x 63.8175 cm, and those of the fuel meat are 0.0508 cm x 6.23316 cm x 60.96 cm. The core is loaded in total with 270 fuel plates, each of which contains about 13.9 g U-235. Each control assembly consists of 6 fuel plates and a pair of 7 wt% boron-aluminum poison blades with aluminum followers providing reactor control. The centrally located transient assembly also consists of 6 fuel plates and two aluminum blades with poison follower blades. Transient power excursions were produced in the core by rapidly ejecting the partially inserted transient rod from

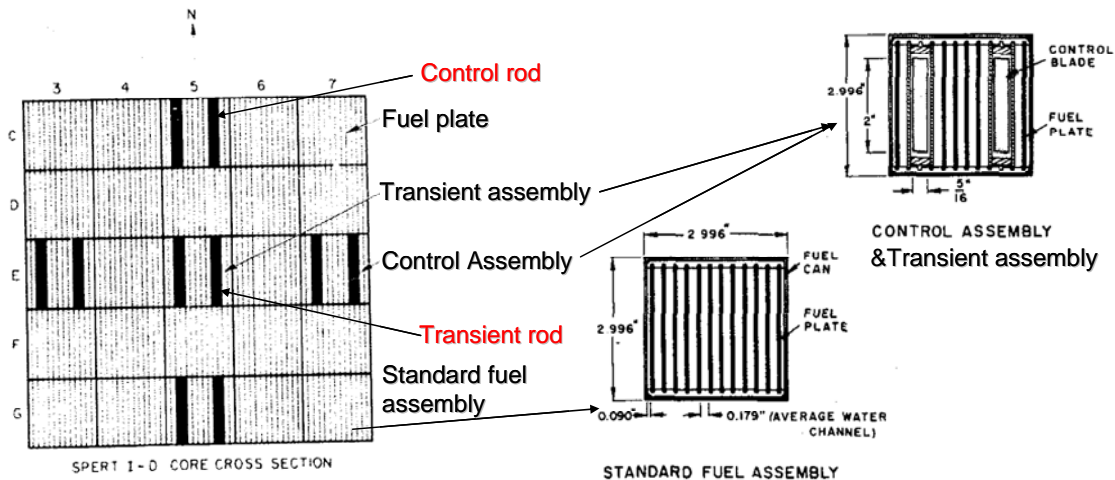


Figure 3. A cutaway view of the SPERT I D-12/25 core cross section and the view of the fuel, control, and transient assemblies (Ref. 11).

the core within about 80 to 120 msec, while the core was at a very low power level (usually less than 10 watts). By this means, an almost step-wise increase of reactivity occurs in the reactor, with the amount of reactivity being predetermined by a measured displacement of the control rods above their normal critical position. More detailed information on this SPERT I D-12/25 has been explained in Reference 11.

Among the SPERT I D-12/25 tests, three of them - conducted with rather short periods of 5.0 msec, 4.6 msec and 3.2 msec - resulted in both thermal distortion of the plates and fuel plate melting while other tests with rather larger periods did not show fuel plate failures. Therefore, the three disruptive tests have been chosen as the benchmark tests to verify the validity of SIMMER-III on simulating this kind of disruptive transient in a light water cooled thermal reactor core with plate-type fuel due to reactivity insertion. In the three tests the inserted reactivity was 2.63\$, 2.72\$ and 3.55\$, respectively. The three power excursion tests with different periods showed similar transient developing mode. SIMMER-III has well simulated transients of the power, released energy as well as temperatures in all the three cases. The results of the tests with a period of 3.2 msec will be described in detail in the following sections.

3.2 SIMMER-III Model of the SPERT I D-12/25 Core

SIMMER-III is a two dimensional code, therefore, the rectangular SPERT I D-12/25 three dimensional core has been reshaped into a cylindrical RZ geometry for the simulations. A further numerical investigation of the core behavior might be carried out in the future with a simulation by the three dimensional code SIMMER-IV [13, 14]. Fig. 4 shows the geometrical model of the SPERT I D-12/25 core in the SIMMER-III simulation. The 25 assemblies are divided into 5 rings according to their symmetry characteristics. After testing of many different kinds of subdivision

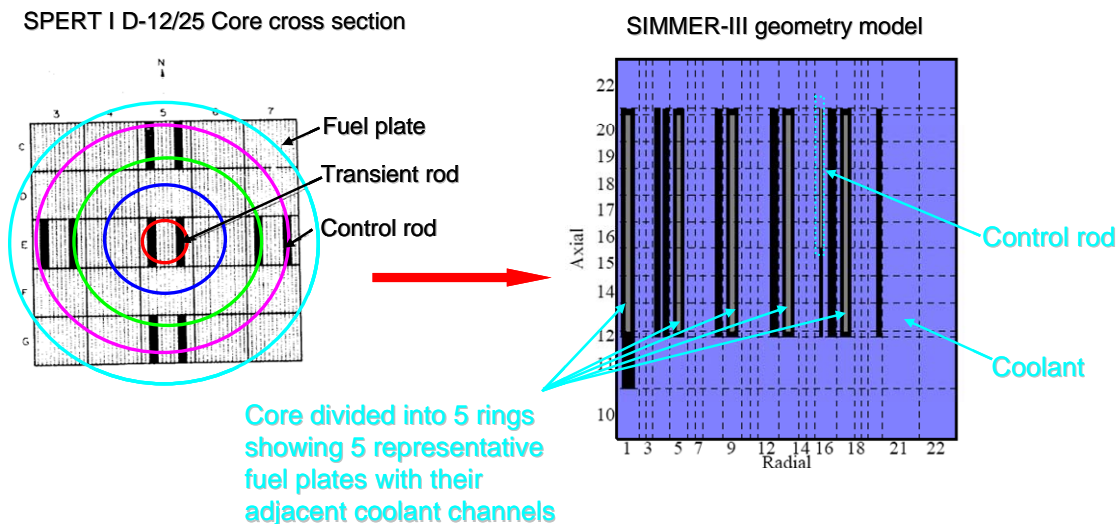


Figure 4. Geometrical model of the SPERT I D-12/25 core in the SIMMER-III simulation.

combinations, the dividing scheme shown in Fig. 4 has been considered to be an optimal one and has eventually been adopted in the simulations, although there are still some aspects having to be omitted by representing the three dimensional rectangular SPERT core in a two-dimensional-geometry. The transient assembly at the core center (position E5, see Fig. 3) is modeled as the innermost ring, its neighboring eight standard fuel assemblies are put in the second ring, standard fuel assemblies at positions C4, C6, D3, D7, F3, F7, G4 and G6 (see Fig. 3) form the third ring, the four control assemblies are arranged as the fourth ring, and the left four standard fuel assemblies are modeled as the fifth ring.

In order to well simulate the water temperature (especially that of the water close to the fuel surface, which is of importance to determine the negative reactivity feedback introduced to the core) each ring shown in Fig. 4 has been further subdivided into 4 meshes in the radial direction. Generally only the first radial mesh includes fuel. For the fourth ring shown in Fig. 4, as it includes both fuel and control rod, the fuel and control rod are then defined in different radial meshes because in SIMMER-III fuel and control rod cannot be placed in the same mesh cell. The validity of this kind of ring and water subdivision method adopted as an approximation in the simulation of the water cooled reactor can be referred to the work of Wilhelm et al. [8].

As explained, the control rod is modeled in the 4th radial mesh of the fourth ring which is close to the real position of the control rod in the SPERT I D-12/25 core. However, in SIMMER-III simulation, the control rods are modeled in the core as one control ring which would introduce too much neutron poison to the core comparing to the real physical core. Non-ring-wise treatment of the control rod can only be realized in future investigation with SIMMER-IV. Therefore, in order to improve the neutron performance as much as possible, the inventory of the poison has been adjusted to a certain value on the basis of the experimental result that the available excess reactivity of the core is about 8.2 \$ from all the control rods. For the initial critical state, the control rod is defined to be withdrawn from the core by 9.2 inches as reported in Reference 11. For the transient case, the reactivity was inserted in the experimental test to the core with the movement of the transient rods in the core center. In the current simulation, this kind of movement has not been modeled. Instead, the transient rods are defined to be out of the core, and reactivity insertions in all cases are introduced to the critical core with a definition of the specified reactivity ramp in the SIMMER-III input file.

In the SPERT I D-12/25 core, each standard fuel assembly has 12 fuel plates, and water channels between these fuel plates are about 4.5 mm wide. The neutron transport in the core has been simulated by employing a homogenized model. Influence of heterogeneity would be of interest in future investigations. For the neutronics calculation, each ring was considered as one region with the same neutron cross-section over the four radial meshes. In other words, isotopes and their properties are well mixed and averaged inside each ring except for the ring with the control rod in which the mesh with the control rod is separated from the other three radial meshes in order not to overestimate the effect of the control rod. With this definition, the neutron flux distribution was reasonably simulated as shown in Fig. 5. In the current SPERT simulations, 40 energy group XS libraries (with 10 groups below 1 eV) generated by means of the C⁴P code and data system [15] have been adopted. More detailed investigations and discussions of key kinetic parameters in the neutronics model can be found in Reference 16. Fig. 5 shows the neutron flux distribution of the 40th energy group which is considered representative for the thermal neutron

flux distribution in the SPERT reactor core.

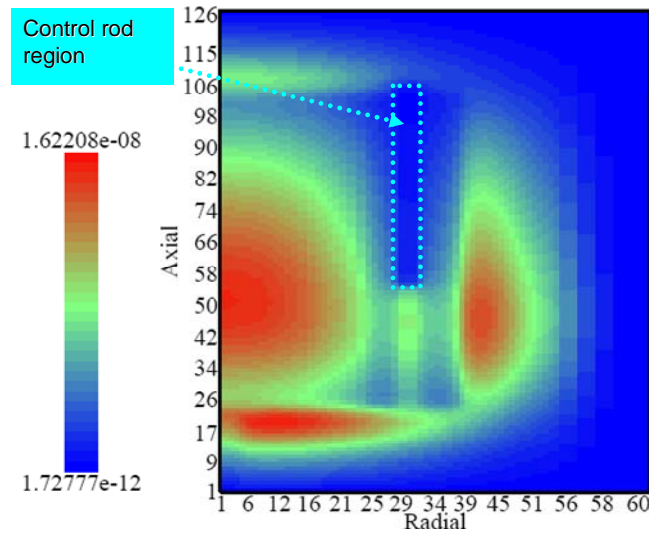


Figure 5. Neutron flux distribution in the core represented by that of the 40th energy group.

3.3 Simulation Results of the Initial Low-power State

Before going into the analyses of transient cases, the analytical model for the initial critical state needs to be well established in the SIMMER-III simulation. Besides the geometrical size of the core, the neutron performance has been compared to the experimental results. Table III shows a comparison of some key parameters between the simulated and experimental results. It shows that SIMMER-III inputs the correct fuel/coolant properties into the simulation. Table III also shows that there is some difference between the measured and calculated values for the reduced prompt generation time ($l/\bar{\beta}$); however, further detailed investigation on these kinetic parameters indicates that these differences can be reduced by applying a more refined model. The prompt neutron generation time, the delayed neutron fraction and the corresponding reduced prompt neutron generation time ($l/\bar{\beta}$) were calculated with MCNP (2D and 3D), ERANOS (2D by BISTRO and 3D by KIN3D), SIMMER-III and compared with the experimental results [16]. Results of the mentioned codes and modeling options provide a coherent picture. The reduced prompt generation time computed by SIMMER-III with adjoint weighting function shows a discrepancy of only about 3% with respect to those of ERANOS/KIN3D.

In the SPERT experimental tests, the steady-state neutron flux distribution was determined from activation of 29 cobalt wires located in the core as shown in Fig. 6. Neutron flux profiles in the A-B and A-C directions normalized on the basis of the maximum flux were reported. The maximum flux was determined to be in the position E-5-5 at about 8 inches from the bottom of

the core. Here E-5-5 means the 5th water channel numbered from the west or left side of the fuel assembly in the E-5 grid position [11].

Table III. Key parameters in the initial state compared to the experimental data

Parameters	Unit	SPERT I D-12/25 Exp.	SIMMER-III
Core cross section	m ²	0.145	0.145
Fissile fuel mass (U-235)	kg	3.8	3.793
Fertile fuel (Al+ U-other isotopes)	kg	13.2006	13.1411
Water mass in the core	kg	51.9	57.3
Water volume in the core	m ³	0.05244	0.05695
Metal volume/water volume		0.66	0.63
K-eff		N/A	1.0005
$\bar{\beta}$	pcm	N/A	841
Reduced prompt lifetime ($l/\bar{\beta}$)	ms	8.16	6.52

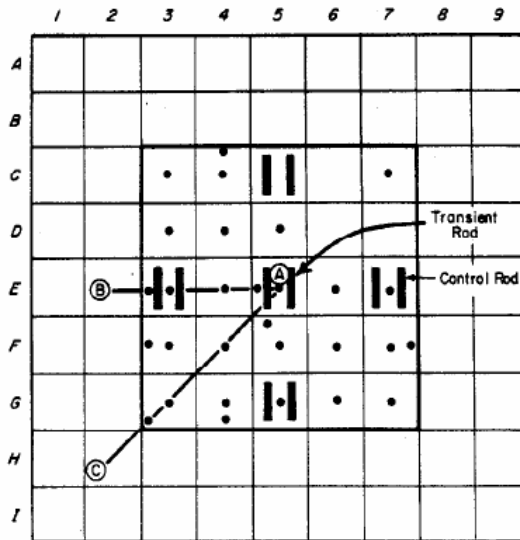


Figure 6. Flux wire activation positions (Ref. 11).

Figs. 7 and 8 show comparisons of the normalized axial and horizontal flux profiles, respectively. As in the experiment, the simulated maximum flux occurs at about 8 inches from

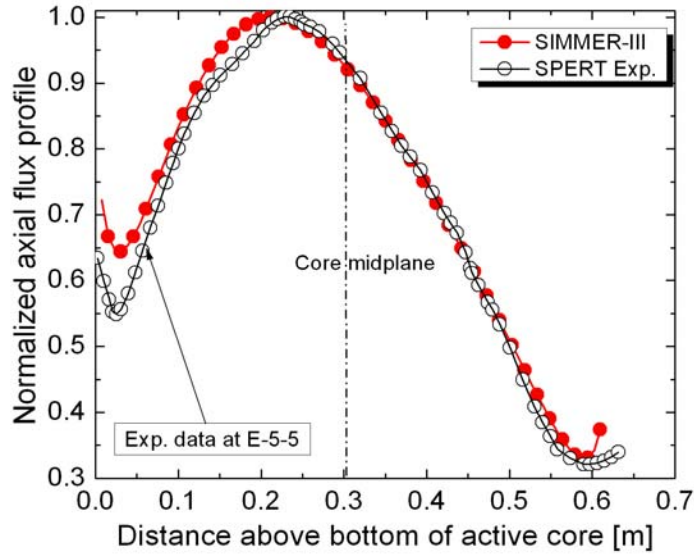


Figure 7. Normalized axial neutron flux profile at the core center.

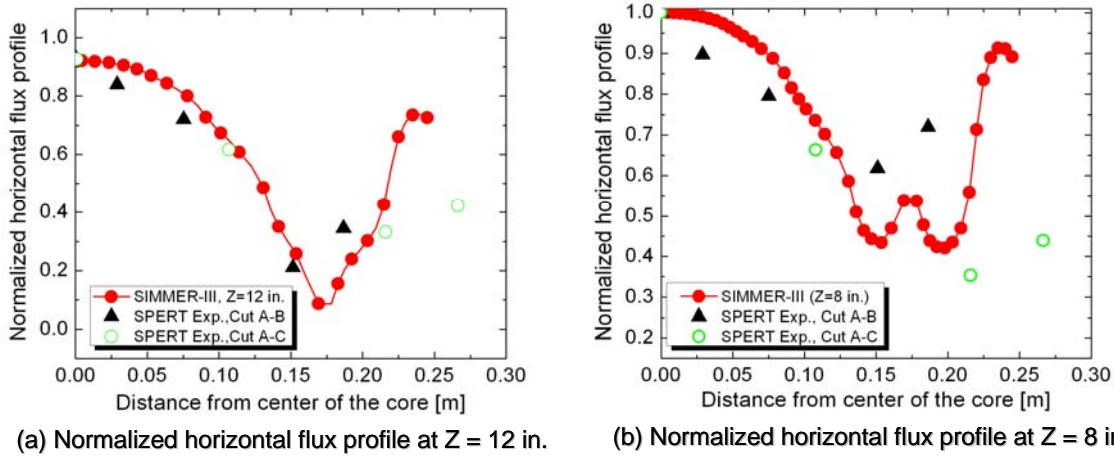


Figure 8. Normalized horizontal neutron flux profiles at specified axial position. Half-width of the rectangular core is about 0.19 m.

the bottom of the core at E-5-5. This is because the control rod is withdrawn 9.2 inches from the core (see Fig. 4) and there is control poison at the core midplane in the radial direction. The simulated axial neutron flux profile shows a very good agreement with the experimental result. Representing the flux shape reasonably well in the center part of the core is a basis to obtain a reliable simulation of the phenomena that happened in the transient cases. Although there are some obvious differences for positions distant from the core center by more than 0.2 m in Fig. 8, considering that the half-width of the SPERT core is about 0.19 m, we can conclude that in the

most important core region, neutron flux profiles have been reasonably well represented. Fig. 9 shows the reactivity loss in \$ as a function of the voided fraction of core moderator. The SIMMER-III simulated results are slightly larger than the experimental ones.

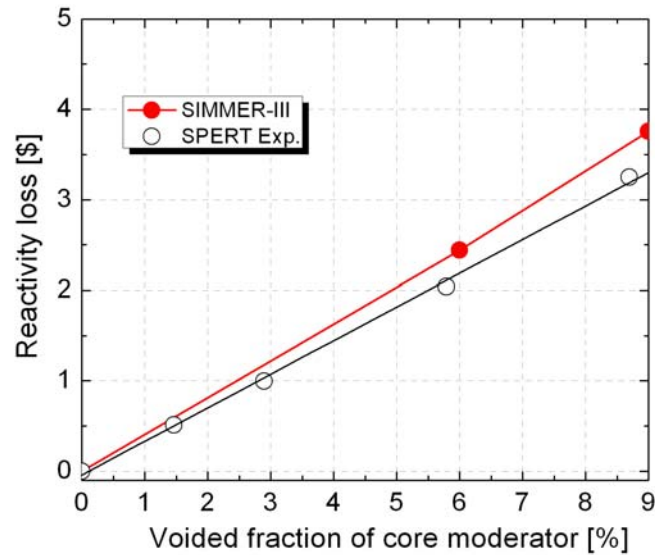


Figure 9. Reactivity loss as a function of void fraction for a uniform distribution of voids.

3.3 Simulation Results of the SPERT Case With a Period of 3.2 msec

On the basis of the well established model for the initial low-power state, analyses for the transient tests have been performed. The power, released energy, and reactivity compensation have been calculated as a function of time and compared with the corresponding experimental values. In several initial simulations, the reactivity compensation before the peak power time has not been sufficient and much higher peak powers had been obtained. This was later found to happen because the fuel dilatation [17] had not been taken into account suitably. With a definition of fuel meat volume change of 0.095% for a temperature increase of 1 K, the reactivity compensation at the peak power time came close to the experimental results and so did the power and released energy. Because the three disruptive tests with periods of 5.0 msec, 4.6 msec and 3.2 msec showed a similar trend, only results for the case with a period of 3.2 msec will be discussed here while SIMMER-III has equally reasonably simulated the other two cases.

In the case with the reactor period of 3.2 msec, 3.55 \$ reactivity was inserted to the core within about 0.12 s. Table IV shows results of the reactivity compensation on the basis of conventional reactivity feedbacks at the peak power time, the peak power, and the released energy. The SIMMER-III results are close to the corresponding experimental values. Fig. 10(a) shows the comparison of the normalized computed reactor power with experiment. Here the normalized

value follows the figure in the SPERT report [11]. Fig. 10(b) shows the comparison of the released energy. In both figures, the peak power time is defined to be the time zero of the experimental and calculated curves. The calculated power and energy profiles exhibit in general a good agreement with the experimental profiles.

Table IV. Key results of the SPERT case with a period of 3.2 msec

TEST with a period of 3.2 ms	Unit	Exp.	SIMMER-III
Reactivity inserted to the core	\$	3.55	3.55
Reactivity compensation at peak power time	\$	2.55	2.52
Peak power	MW	2250	2575
Energy release at the time of peak power	(MW-sec)	13.8	15.88
Total energy release	(MW-sec)	30.7	34.36

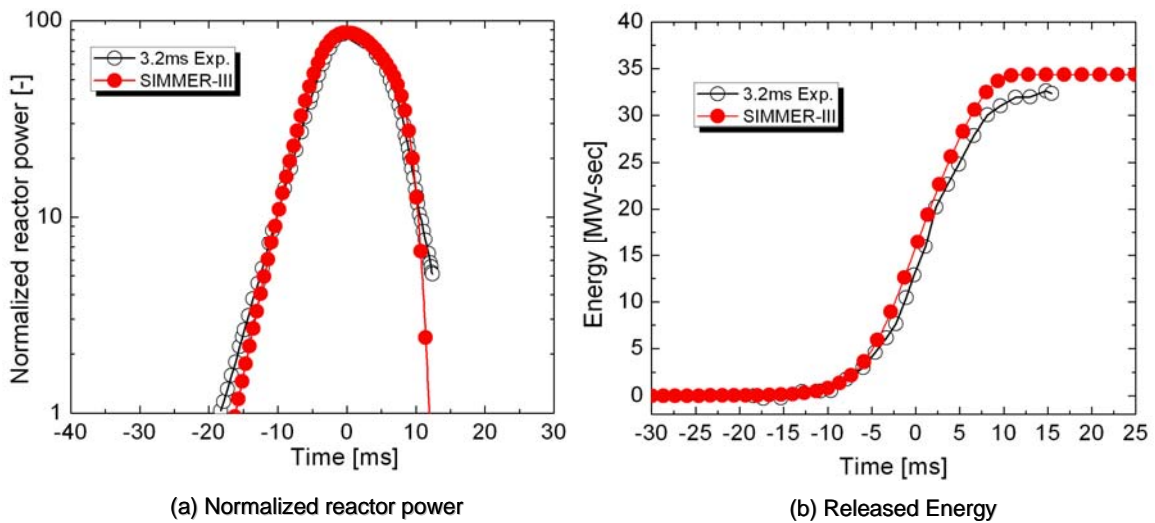


Figure 10. Transients of the normalized reactor power and the released energy.

Fig. 11 shows the comparison of temperatures at location of C7 (9E) 0. Temperature at this location is chosen for comparison because at the end of this test only the fuel plates in C3, C7 G3 and G7 partially remained at their original positions while others together with the thermocouples inside were destroyed. C7 means the fuel assembly at C7 grid position (see Fig. 3). 9E stands for the East-side of the 9th fuel plate starting from the left hand side of the fuel assembly and 0 means vertical center of the core. The experimental surface temperature was a measured value but the meat center experimental temperature shown in Fig. 11(b) was reported to be calculated from the surface temperature. The SIMMER-III simulated meat center

temperature agrees well with the reported values although there is some difference existing in the surface temperature.

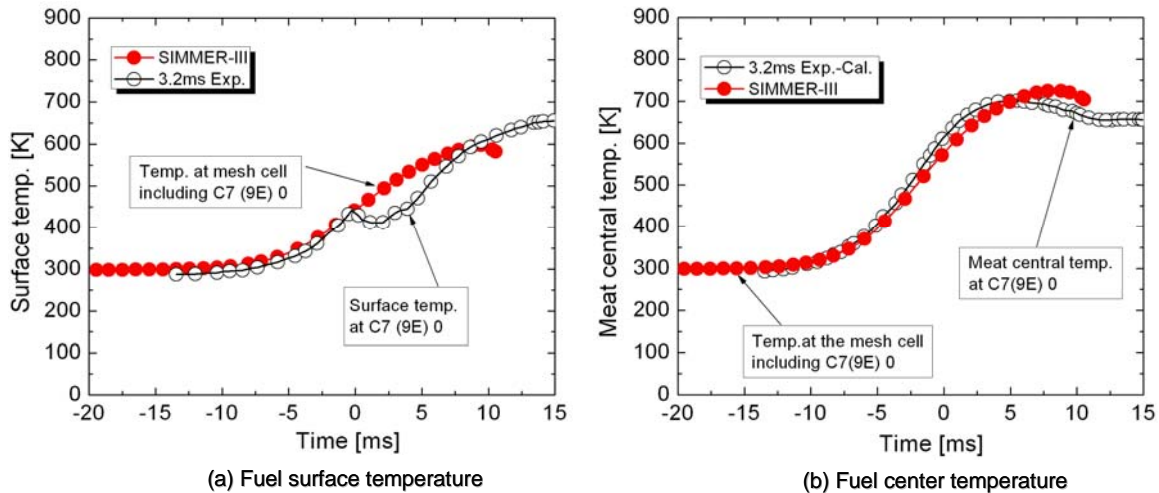


Figure 11. Transients of the fuel surface and center temperatures.

4. CONCLUSION

The SIMMER-III code has been extended to simulate specific core disruptive accident scenarios in water-moderated thermal test reactors. A plate-type fuel model has been implemented to the multi-physics code SIMMER-III, and this new model has been verified to be able to simulate fairly well the temperature profile of the plate-type fuel. With this plate-type fuel model, SIMMER-III simulations on SPERT I D-12/25 tests have been performed considering the possible feedback effects from voiding and fuel plate expansion. The simulated results are qualitatively reasonable both in the initial low-power state and in the three short time excursion tests. Comparison with experiments reveals that there is still space for further modeling improvements. Modeling of negative feedback mechanisms just before and after the peak power point needs further attention and more specific analyses of the negative feedback contribution from fuel dilatation, radiolytic gas formation, sub-cooled nucleate boiling, thermal expansion, and steam formation is of further interest. The arrangement of the control assemblies in the two dimensional RZ geometrical model needs further improvement. In addition, the effect of heterogeneity may need to be taken into account properly with respect to neutronics in future simulations.

REFERENCES

1. Sa. Kondo, et al., "SIMMER-III: an Advanced Computer Program for LMFBR Severe Accident Analysis," *Proc. Int. Conf. on Design and Safety of Advanced Nuclear Power*

- Plant (ANP'92)*, Vol. IV, pp. 40.5.1-40.5.11, Tokyo, Japan (1992).
2. H. Yamano, et al., SIMMER-III: a Computer Program for LMFR Core Disruptive Accident Analysis -Version 3A Model Summary and Program Description. *JNC TN9400 2003-071*, Japan Nuclear Cycle Development Institute (2003).
 3. Y. Tobita, Sa. Kondo, et al., "The Development of SIMMER-III, an Advanced Computer Program for LMFR Safety Analysis, and its Application to Sodium Experiments," *Nucl. Tech.* **153** (3), pp. 245-255 (2006).
 4. H. Yamano, et al., "SIMMER-III: a Coupled Neutronics-Thermohydraulics Computer Code for Safety Analysis," *15th Int. Conf. on Nucl. Eng.*, Nagoya, Japan, April 22-26 (2007).
 5. W. Maschek, A. Rineiski, et al., "The SIMMER Safety Code System and its Validation Efforts for Fast Reactor Application," *PHYSOR 2008*, Interlaken, Switzerland, September 14-19 (2008).
 6. W. Maschek, et al., "SIMMER-III and SIMMER-IV Safety Code Development for Reactors with Transmutation Capability," *M&C 2005*, Avignon, France, Sept. 12-15 (2005).
 7. Y. Tobita, Sa. Kondo et al., "Space-time Kinetics Simulation of an Early Burst Phase of the Criticality Accident," *Int. Workshop on the Safety of the Nuclear Fuel Cycle*, Tokyo, Japan, May 29-31 (2000).
 8. D. Wilhelm, G. Biaut, Y. Tobita, "SIMMER Model of a Low-enriched Uranium Non-power Reactor," *Nuclear Engineering and Design*, **238**, pp. 41-48 (2008).
 9. G. Biaut, J. Couturier, D. Wilhelm and P. Liu, "Upgrading of the Coupled Neutronics-fluid Dynamics Code SIMMER to Simulate the Research Reactors Core Disruptive RIA," *PHYSOR 2008*, Interlaken, Switzerland, Sept. 14-19 (2008).
 10. K. Kamiyama and Sa. Kondo, SIMMER-III Structure Model –Model and Method Description, *JNC TN9400 2004-043*, Japan Nuclear Cycle Development Institute Report (2004).
 11. R.W. Miller, Alain Sola and R. K. McCardell, Report of the SPERT I Destructive Test Program on an Aluminum, Plate-type Water-moderated Reactor, *IDO-16883* (1964).
 12. K. Woods et al., "SPERT-D Aluminum-clad Plate-type Fuel in Water, Dilute Uranyl Nitrate, or Borated Uranyl Nitrate," *NEA/NSC/DOC (95)03/II HEU-MET-THERM-006* (1995).
 13. H. Yamano et al., SIMMER-IV: a Three-dimension Computer Program for LMFR Core Disruptive Accident Analysis -Version 2A Model Summary and Program Description. *JNC TN9400 2003-070*, Japan Nuclear Cycle Development Institute (2003).
 14. H. Yamano et al., "Development of a Three-dimensional CDA Analysis Code: SIMMER-IV and its First Application to Reactor Case," *Nuclear Engineering and Design*, **238**, pp. 66-73 (2008).
 15. A. Rineiski, V. Sinitsa, W. Maschek, "C4P, a Multigroup Nuclear CCCC Data Processing System for Reactor Safety and Scenario Studies," *Jahrestagung Kerntechnik 2005*, Nuremberg, Germany, May 10-12 (2005).
 16. F. Gabrielli et al., "Neutronics Model for SPERT," *Jahrestagung Kerntechnik 2009*, Dresden, Germany, May 12-14 (2009).
 17. K. Yanagisawa et al., "Dimensional Stability of Low Enriched Uranium Silicide Plate Type Fuel for Research Reactors at Transient Conditions," *J. Nucl. Sci. Tech.* **29**[3] pp. 233-243 (1992)